

## CHARACTERIZATION OF A SYNTHETIC FEMUR WITH THE EMPLOYMENT OF THE FINITE ELEMENT METHOD AND VALIDATION BY OPTICAL EXTENSOMETRY

**Leandro Zen Karam, lekaram@cpgei.ct.utfpr.edu.br**

Federal University of Technology – Paraná, Avenida 7 de Setembro, 3165, 80230-901 Curitiba, Paraná, Brazil

**Jean Carlos Cardozo da Silva, jeanccs@utfpr.edu.br**

Federal University of Technology – Paraná, Campus Pato Branco, Via do Conhecimento, Km 1, 85503-390, Pato Branco, Brazil

**Leandro de Marchi Pintos, leandro.eie@gmail.com**

Federal University of Technology – Paraná, Campus Pato Branco, Via do Conhecimento, Km 1, 85503-390, Pato Branco, Brazil

**Leandro Grabarski, grabarski@cpgei.cefetpr.br**

Federal University of Technology – Paraná, Avenida 7 de Setembro, 3165, 80230-901 Curitiba, Paraná, Brazil

**Lídia Carvalho, lidia.carvalho@ipsn.cespu.pt**

IPSN - Instituto Superior de Ciências da Saúde - Norte - Rua Central de Gandra, 1317, 4585-116 Gandra PRD, Portugal

**Hypolito José Kalinowski, hjkalin@cpgei.ct.utfpr.edu.br**

Federal University of Technology – Paraná, Avenida 7 de Setembro, 3165, 80230-901 Curitiba, Paraná, Brazil

**Abstract.** *In this work it is reported the use of fiber Bragg grating sensors for the validation of a numerical model (finite elements method) of a synthetic femur, produced by Sawbones<sup>®</sup>. The model is developed after a numerical model already used at the University of Aveiro. For the experimental validation a system for setting and implementation of load steps in the synthetic bone is developed, where the forces are applied in close similarity to those in the human femur in standing position. The results of the FEM numerical simulation are similar to results published in the literature. The experimental results are satisfactory and validate the numerical model. Another synthetic femur was fractured in 45° of the medial third, and it was used for fixing a osteosynthesis plate with the corresponding screws, provided by Synthes<sup>®</sup> Company. The fractured femur has been tested experimentally, and a numerical model is used to compare with the previous essay in similar conditions. We observed a strain concentration around the hole of the osteosynthesis plate, on the exact spot of the out break of the fracture, and the strains is about ten times larger than the strains in the region between the holes, about 1.5 mm from apart. Thus, the positioning of the osteosynthesis plate during cirurgical intervention is of fundamental importance in the fracture healing process.*

**Keywords:** *Synthetic femur; osteosynthesis plates; optical fiber sensors; fiber Bragg gratings; finite element method; fracture fixation*

### 1. INTRODUCTION

Aristotle, in *Parts of Animals* wrote, “Large animals need large, strong and rigid basis supports, especially those who have particularly very wild habits for living”. This sentence shows that since Antiquity, the relations between body dimensions and level of activity are observed. However, the correlation between mechanical load and the architecture of living tissues was only discussed many centuries after that. Wolf, in 1892, suggested that the orientation of trabeculae in bone like the rigidity of a femur corresponds to the trajectories of maximum stresses. The geometric orientation in space would be obtained through a process of adaptation, observed and studied by Roux. In 1881, he considered that bone adaptation is the result of a mechanism of self-regulation, where it is possible to obtain maximum performance with minimum work. That process of mechanical adaptation is observed not only in the muscle-skeletal system but also in others tissues.

The knowledge of the influence of mechanical stimulus in the process of cell differentiation in living tissues is fundamental for different subjects in health sciences. Regarding the great number of factors evolved in the process of mechano-regulation, it is hard to science to rise up the many questions related. Meanwhile, another approach was made, beyond the theoretical and experimental ones (Kelly, 2008). This new approach, called computational biomechanics, makes use of computational means, by employing the finite element analysis (FEM) (Huiskes *et al.*, 1983; Prendergast, 1997). This method has a great potential because in an easy way, is possible to make several analysis for different geometries, loads cases and material properties. However, computational limitations and the complexity and the difficulty to determine the material properties of living tissues turns necessary the use of simplified computational models. For example, to apply an external load to a bone, it is assumed that bone has linear elastic properties and then is possible to use commercial software to model bone behavior (Prendergast *et al.* 1996; Wu *et al.* 1998).

The finite element analysis consists in dividing the overall domain of interest into several sub-domains, each one called finite element (Carrer, 2006). Then, for each finite element the local behavior is described using simple functions. In this method, are used local approximations instead of global ones, to achieve a solution for the problem.

Beyond the advantages of computational biomechanics, this method gives more control on the problem but also a large power of abstraction and it is necessary to validate the numerical results with experimental ones. After the validation of the numerical model, it is possible to use it for others load cases and material properties.

Experimental techniques have been used largely in biomechanic applications, measuring loads, stresses and strains in bone structures. The most conventional methods of analysis of tensions and displacements at the surfaces are photoelastic or interferometric holography techniques, strain gauges, dial gauges and other mechanical and electrical sensing devices. Those experimental techniques can be very accurate and sensitive; however they give lack of information because is only in limited regions of the structure. The technology of optical fiber sensors have progressed quickly in the last decade. Fiber optic sensors are characterized by their high sensitivity when compared to other types of sensors. They present some interesting advantages such as their compactness, wide bandwidth, immunity to electromagnetic noise, versatility of its geometry, low cost and possibility of remote sensory system (Othonos and Kalli, 1999).

The optical fiber sensors had a great development, since the half of the past century, with a large number of studies in the area of communications. With the discovery of photosensitivity by Hill and its co-workers in 1978 (Hill *et al.* 1978), stimulated the application of optical fibers as sensory systems.

The fiber Bragg gratings (FBG) are based on the property of modifying permanently the refractive index of the core, by the absorption of ultraviolet light (UV). The periodic modulation of the refractive index acts as selective filter of wavelengths, that satisfy the Bragg condition, obtaining thus the fiber Bragg gratings (Hill *et al.*, 1978). Due to their properties, FBG can be used as sensors in areas such as materials, civil and biomedical structures.

The fiber Bragg grating sensors are based on the measurement of the peak shift of the Bragg wavelength,  $\lambda_B$ , when subjected to the action of external parameters, such as mechanical stress and temperature (Kersey *et al.*, 1997). For a FBG under longitudinal mechanical stress the peak shift of the Bragg wavelength,  $\lambda_B$ , may be calculated as:

$$\Delta\lambda_B = 2 \left( \Lambda \frac{\partial n_{eff}}{\partial l} + n_{eff} \frac{\partial \Lambda}{\partial l} \right) \Delta l + 2 \left( \Lambda \frac{\partial n_{eff}}{\partial T} + n_{eff} \frac{\partial \Lambda}{\partial T} \right) \Delta T \quad (1)$$

The first term corresponds to the strain effect of the FBG, and the second term corresponds to the displacement of the wavelength of Bragg due to thermal expansion (Othonos, 1997).

In the present work are used FBG sensors, to assess the strain pattern at the surface of femurs. These results, validated by numerical ones, are important to give more scientific information about the healing and bone remodeling process associated to bone fractures. The knowledge of these mechanisms can be very important in the development of new and more adequate therapeutical techniques as also to supply previous results of bone response to the implantation of fracture fixation device. However, there are several characteristics of extreme complexity evolved in this process that should be taken into account (Zhang *et al.*, 2005).

The processes of bone fracture fixation have been exhaustingly studied in the last years, due to its great socio-economic impact. The main objective of the internal fixation devices, as well as the new techniques of fixation of bone fractures, is to reach, in the fastest way, the total functionality of the member (Ruedi and Murphy, 2002). The osteosynthesis plates are mechanical devices manufactured with materials of high rigidity. Apparently, is desirable and necessary that the fixation device allows the load transmission, generating a micromobility that stimulates the bone remodeling process necessary to the healing of fracture (Ruedi and Murphy, 2002).

The general objective of this work is to develop a system, based on optical extensometry, for the validation of three-dimensional numerical models of intact and broken femurs, made in FEA.

## 2. MATERIALS AND METHODS

For this study it was used three synthetic femurs from Sawbones<sup>®</sup> (fig. 1) and developed by Pacific Research Labs<sup>®</sup>. These products are being developed for academic studies, since 90's and they are manufacture with materials that replicate the properties of a natural integer femur under mechanical load. The results obtained from the mechanical tests were validated by Chong, 2007 as it is observed in figure 1.

Heiner, 2008, carried out a structural validation of femur of fourth generation (with the new materials). In their study they have used six femurs, tested under several load conditions. The obtained results in the study clarify the role of mechanical properties of the product. Ramos, 2007, developed a new model of total hip prostheses: for the experimental studies prototypes were implanted in synthetic femurs, in order to simulate the bone mechanical behavior, after surgical procedure. McNamara *et al.*, 2006, also used synthetic femurs to compare types of glue and load mechanisms transfer, in total hip prostheses. Mehlman, 2006, carried out studies that compare the behavior of femur when is fixed with intra-medullar devices and plates of osteosynthesis, using femurs from SAWBONES<sup>®</sup>.

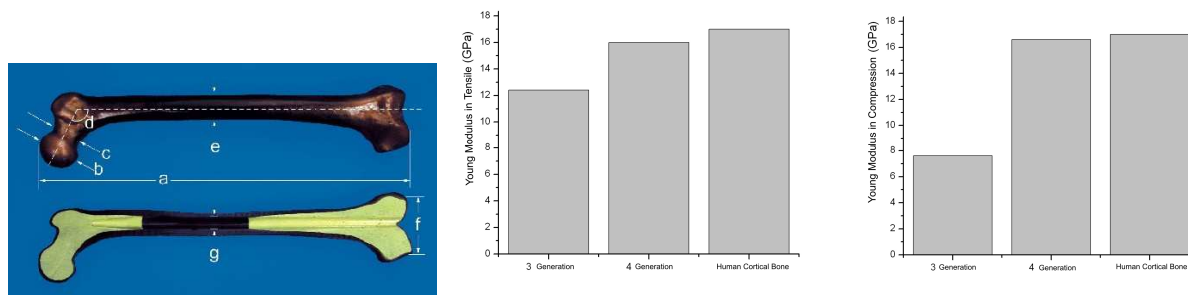


Figure 1: Comparison between the composite of 3rd and 4th generation when subjected to tensile and compression tests. (Heiner, 2008) and developed by synthetic bone Sawbones® a) 455 mm b) 45 mm c) 31 mm d) 135 and) 27 mm f) 74 mm g) 13 mm

The model used within this study, was model #3403 from Sawbones®. This work was sponsored by SYNTHES®, for the supply a set of plates with the same geometry and different materials. For the osteosynthesis plates were considered eight specific screws and for the materials were considered stainless steel (316L) and an aluminum, titanium alloy and niobium (TAN). The properties of the materials are listed in table 1 (results obtained with mechanical tests and present in section 3.2.1).

Table 1: Comparison of materials properties, used for the osteosynthesis plates produced by the SYNTHES®.

	Stainless Steel	Niobium TAN
Strenght Stress	860 MPa	900 MPa
Yielding Stress	690 MPa	800 MPa
Strain	12%	10%
Density	8 g/cm <sup>3</sup>	4.52 g/cm <sup>3</sup>
Young Modulus	200 GPa	110 GPa

The supplied plate was LC-DCP® (Limited Contact Dynamic Compression Plate) (figure 2). It possesses a complex geometry in the inferior part and for that reason, diminishes the contact surface between the metallic plate and bone surface, where it will be implanted.



Figure 2: LC-DCP® produced by SYNTHES®.

For the mechanical test, it was used a plate with twelve holes. The length of the plates varies according to the number of holes: 106 mm length has six holes; 214 mm length has twelve holes. The other dimensions of the plates are standardized: 5.2 mm of thickness, 17.5 mm of width and 18 mm of space between holes.

The surgical procedure of the plate implantation was carried out at the University Hospital of the Cajuru according to the protocol, in Curitiba/PR, for the team of the third year of residents in Orthopedics. Eight screws of 4.5 mm of thickness and 30 mm of length had been used in the surgical procedure. The construction of the fracture was made in the same day, with the use of a specific wimble for hospital use, with a drill of 3.2 mm of diameter. The fracture has an angulation of 45°. A distance of 2.5 mm between bone fragments was left, in order to analyze the mechanical behavior of the osteosynthesis, under a physiological load.

The choice of the type of fracture present in this study, took in account the type of fixation device supplied by the manufacturer. According to Ruedi and Murphy, 2002, for simple oblique fractures with 45° in the medial part of the femur, are indicated fixation devices with plates LC-DCP or intra-medullar devices.

The experimental test was performed at the Federal University of Technological - Paraná, campus Pato Branco, in the Laboratory of Radiofrequency and Electromagnetic Compatibility.

To apply the mechanical loads, it was designed an experimental set up with capacity of 2000 Kgf, for the effect. A load cell from Excel was used as system acquisition, with a sensitivity of 2 mV/V, for the nominal load capacity of 200 kgf.

In the region of the femoral head, a comparator was placed to monitor the longitudinal strains of the synthetic femur, caused from the load mechanism set up. For that reason, it was used a sensor of displacement LVDT of type WA/100 mm from HBM® (Hottinger Baldwin Messtechnik GmbH, Darmstadt, Germany).

For the analysis and measurements of the load and absolute displacements, was used a universal amplifier of measurements QuantumX, MX840, precision class of 0.01 and sample rate up to 19.2 kHz/channel, of company HBM®. The load cell and the sensor of displacement LVDT have been connected to a system of acquisition of QuantumX data, being this last one connected to a PC Intel (R) Core (2 TM) Duo CPU 2.7GHz and 2GB of RAM where the results have been treated and stored with the application of the program Catman Easy/AP Version 2.2 of company HBM®, described previously. The sample rate used for the experiment was 50 Hz and was used a filter Butterworth of 1Hz, implemented in Catman Easy/AP software.

The femur was located at 11° in the frontal plain, simulating an integral human being in the orthostatic position, according to Bergman, 2001. Figure 3 illustrates the experimental set up used in this work.



Figure 3: Test arrangement and instrumentation of the femur

For the experimental set up of intact femur, it was instrumented with FBG's at the surface of the bone, in order to measure the local strains. Twelve multiplexed sensors, recorded in the same optical fiber, have been glued at the surface of the four main faces of the femur (anterior, posterior, distal and medial), at the diaphysaric region, each one with three sensors. They were numbered by their increasing wavelengths, where sensors 1, 2 and 3 are at the anterior face, sensors 4, 5 and 6 are at the lateral face, sensors 7, 8 and 9 are at the medial face and sensors 10, 11 and 12 are at the posterior face. For a better understanding, it is possible to see in figure 4 the right location of the twelve sensors.

For the experimental set up of fractured femur were glued nine sensors; three at the surface of the osteosynthesis plate, four at the bone surface, laterally at the plate and others two in each side of the focus of the fracture. The last two sensors have been exactly located at the opposite face where the plate was located (fig. 4). The places where the sensors have been located were chosen from a preliminary simulation in FEM, where it can be seen the places of biggest values of strain are located. These strain patterns, after the fracture, will indicate the distribution of strains throughout the femur, as well as a possible development of the bone tissue, in the healing process.

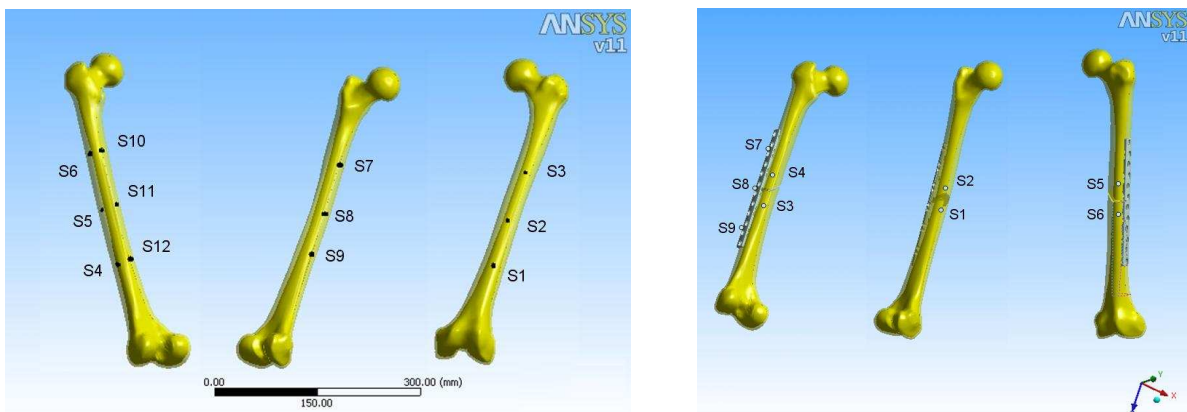


Figure 4: Indication of the position of sensors in the femur and the fractured one.

The wavelength shift of each FBG was acquired by the acquisition system from Micron Optics, Inc., model sm125, and then those values were converted into strain values ( $\mu\text{Strain}$ ). For each load, were performed five measurements, to assure the repeatability system.

Geometry was developed and improved in a partnership between the Federal University of Technology - Paraná (UTFPR) and the University of Aveiro (UA). The geometry previously used by the University of Aveiro, have been acquired together to the *Standardized Femur Program*.

For the numerical study, the geometry was created using the commercial program SolidWorks®. The surfaces of the base have been smoothed at the head of femur, as well as were made corrections in the geometry, to avoid an overlapping of volumes bodies corresponding to trabecular and cortical bones (fig. 5). An interface between trabecular and cortical bones was considered, consisting with the existence of two distinct bodies, one inside of the other.

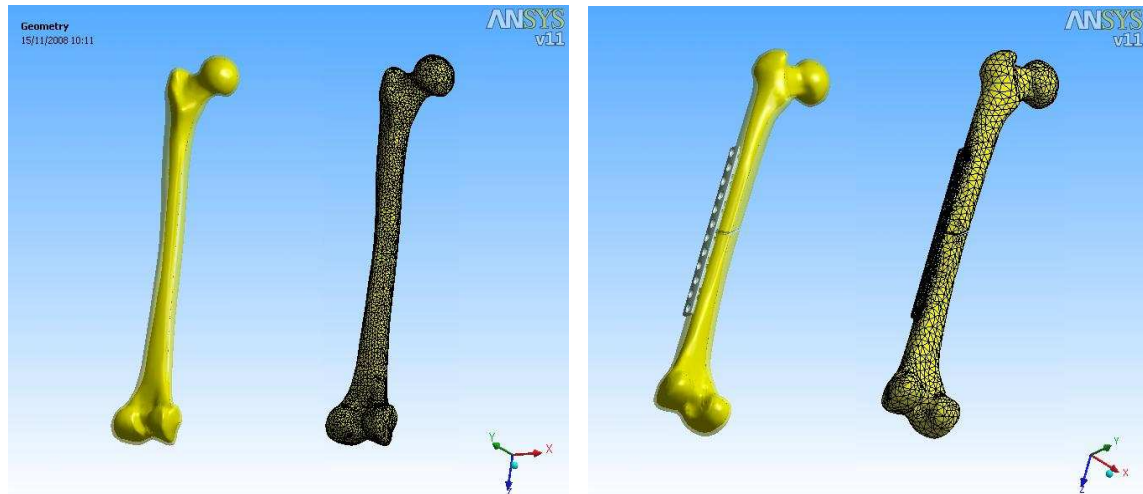


Figure 5: CAD model of the femur after the modifications made and mesh generated by the software ANSYS®.

After all these considerations, the model was exported in the parasolid format into ANSYS® software, version 11.0. As the archive is imported, is generated the geometry of the numerical model and then, it is generated the finite element mesh. The mesh was refined in specific points of interest and to approach the results with the reality, without overloading the system. The used element was SOLID 187, hexahedral. The mesh generated for the model has a total of 38519 elements and 72754 nodes (fig.5).

The plates of osteosynthesis geometry was developed directly in the SolidWorks® software, from measures supplied in catalogues of the products from SYNTHES®.

For the formulation of the numerical model of the broken femur and fixed, was made an assembly of the parts of the model, being carried out also in SolidWorks® software. The assemble geometry with broken femur, osteosynthesis plate and the supports for load application, have been exported in parasolid format and imported by software ANSYS®. A mesh of finite elements was generated, having 59816 nodes and 30989 SOLID 187 elements (fig. 5).

The fixation of the osteosynthesis plate at the bone was made by contact elements, this study don't use screws at the finite element model. The interface between bone and osteosynthesis plate simulate "bonded" conditions.

Inferior and superior supports, used in the mechanical experimental tests, had been modeled in ANSYS® software. The model also was placed in the same way (fig. 5). The used inferior support in the first mechanical assay was simulated in simple way: a fixed support in the same position was created where it was located. For the load application in the superior surface at  $11^\circ$ , the forces were decomposed in axis Y and Z. For the second experimental test with integral femur, it was modeled two parts to simulate the support system. In this in case, the superior support already was inclined in  $11^\circ$ , not needing to decompose the forces.

With all the parts in right position, the loads have been applied at the superior part (fig 6). The applied loads are the same ones of the experimental test, in order to validate the model. The applied loads considered were: 200N, 400N, 600N, 800N and 1000N for integral femur and 20N, 40N, 60N, 80N and 100N for broken femur.

### 3. RESULTS AND DISCUSSIONS

The Von Misses stresses give information about where the highest values are and where the sensors are located in the model. When analyzing the results obtained with FEM, it can be seen that the minimum principal strains are located mainly in the medial face of the superior region of femur (fig. 6). In the lateral face of the inferior region of femur, next

the base, it can be seen a region of significant concentration of strains. The point of maximum concentration of strains in compression is at the inferior face at the neck of the femur.

In both figures, it can be seen that in the anterior and posterior faces of bone, there are a great number of small areas with stress concentration, characterizing areas where strain exist, but do not influence in the process of fracture healing.

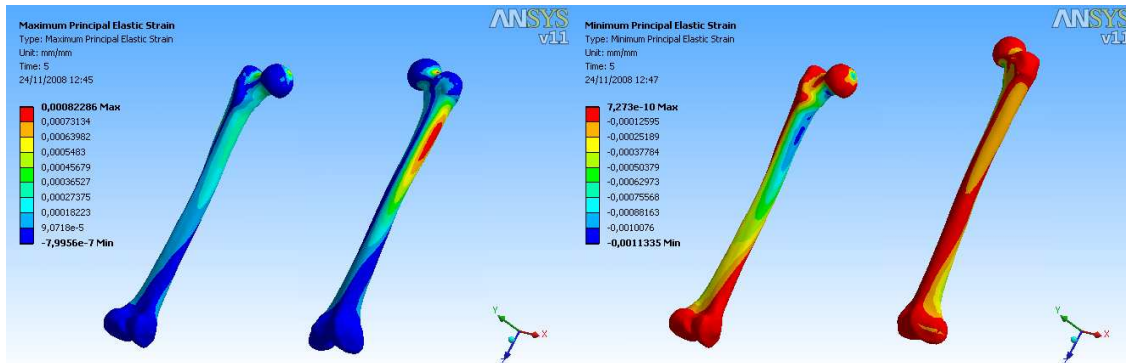


Figure 6: Distribution of maximum principal strain and distribution of minimum principal strain.

Sensors 1, 2 and 3 were located at the anterior face of femur and had detected small variations of strain for all loads (around 150  $\mu$ strain). The data acquired for the sensors located in the lateral face exhibit a variation of 400 to 800  $\mu$ strain. By the other hand, it's the medial face where were registered the great strains of compression related to the positioning of applied load.

Sensor 9, at the beginning of the applied load, presents strains around -200  $\mu$  $\epsilon$  and -700  $\mu$  $\epsilon$  at the end. The same happens with sensor 7, but more intensively. At the beginning of the applied load the strains were around the same values of -200  $\mu$  $\epsilon$  of sensors 8 and 9; at the end, the strains had arrived close to -1100  $\mu$  $\epsilon$ . Sensor 12 presents strains of compression, at the beginning, next to -100  $\mu$  $\epsilon$  and at the end the levels arrived next to -450  $\mu$  $\epsilon$ , that it is approximately half of the strains obtained at the medial face, for example.

The graphs listed in figure 7, present the strains measured by FBG's as well as the strains obtained by FEM.

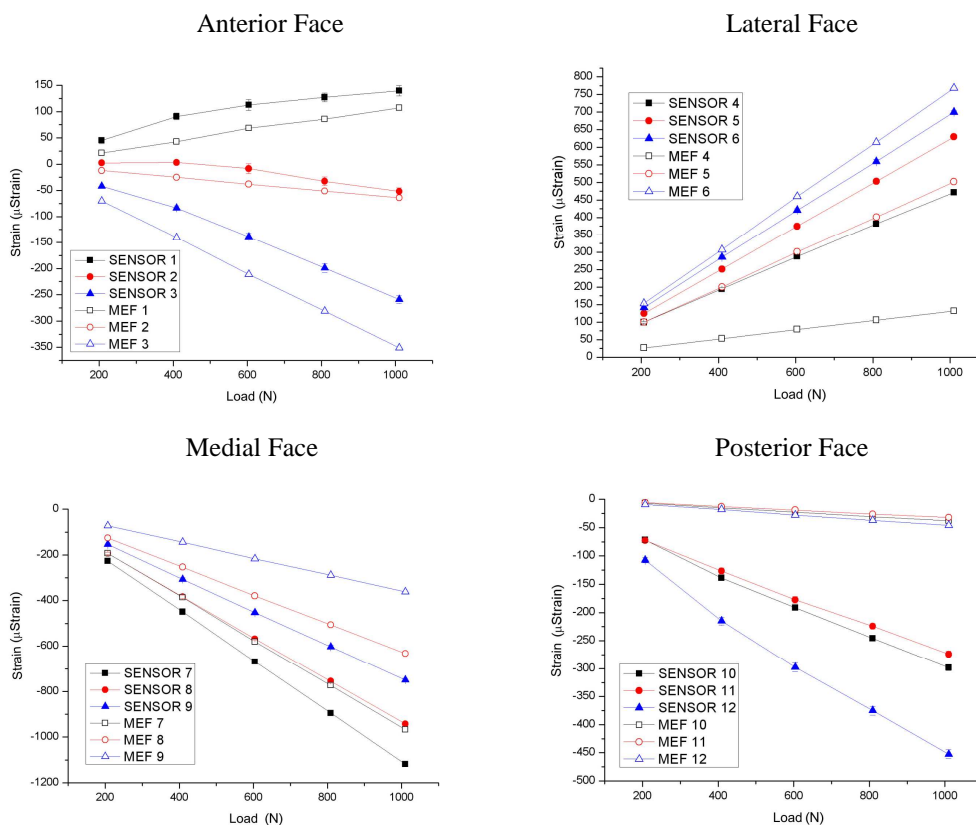


Figure 7: Comparison between the experimental strains on the anterior, lateral, medial and posterior face respectively.

Without considering the specific values obtained by each sensor and observing globally the results, it is possible to say that the two sets of results (numerical and experimental) are in good accordance, not only qualitatively but also quantitatively. The lesser difference is around 10 % and the biggest difference is about 110 %, for an applied load of 1000 N.

An interesting remark is the fact that numerical model was considered linear. However, the experimental model is composed for materials without linear behaviors, when submitted to high loads (viscoelastic behavior). It can be evidenced with the linear progression of the numerical values obtained, while the same is not evidenced in the experimental test, when the material is submitted to highest loads.

The applied loads considered in this study are the same for one integral femur, when considering a human being in orthostatic position, or when is walking (Argenta, 2008). This demonstrates that the measured strains are, without considering biological variables, very close to ones existing in a human femur.

Another very important observation made in the experimental model, was the creep effect, caused by materials properties, during applied loads. In that way, it was established that was necessary to wait around fifteen minutes between loads, to make sure a new come back its initial characteristic. To avoid errors, it was performed ten load cases and with the results was calculated the standard deviation. The biggest standard deviation observed was around 8  $\mu$ strain. According to the results displayed in figure 7, it can be seen that with the increase of the applied load, the numerical and experimental values become less similar, having differences around 20 %.

The comparison between experimental and numerical strains, at the lateral face, also exhibit the large differences for higher values of load, with exception for sensor 4, that had a strain around 450  $\mu\epsilon$  while the numerical model presented a value of 150  $\mu\epsilon$ . In the lateral and the anterior faces, the values obtained, for small loads, are very close. With the increase of loads up to 600 N, the values are close, with a small difference between the two methods.

Comparing the values obtained for higher levels of loads; in the anterior face the differences can reach around 15 % to 20 %. Already in the lateral face this difference falls for about 5 % to 10 %.

An important factor in the validation of results is the difficulty of measuring the strains at the same points, in both methods.

The results obtained in the numerical simulations for the posterior face are in accordance with ones obtained for similar works related in literature (Talaia *et al.*, 2007). However, the strains obtained for the FBG's, in the present work, had been of higher levels, arriving around -450  $\mu\epsilon$ .

The geometry of femur, together with the location of sensors at the posterior face, with a little displacement in position of some millimeters for the medial face, made that was obtained higher values then in the numerical model.

In the experimental tests of Talaia *et al.*, 2007, the strains at the posterior face were inferior to -100  $\mu$ strain, as well as in this work. This demonstrates that the arrangement elaborated for the experimental set up has adequate behavior; and, mainly, that the numerical model is satisfactory, being able to be used for the development of new orthopaedic components or for the analysis of existing components.

The results obtained in numerical simulation are not the best, with a series of adjustments we can close to the experimental test. Screws can be inserted in the FEM model, adjusting the material properties of the numerical model, modifying boundary conditions, the numerical model will have a nonlinear behavior and have behavior closer to the experimental test.

To facilitate the visualization of strains at the same places where the sensors are glued, an image of the minimum principal strains at the medial face of femur was obtained. A bar chart was elaborated, to compare the strains obtained for the numerical simulation and for the experimental tests, as it is showed in figure 8.

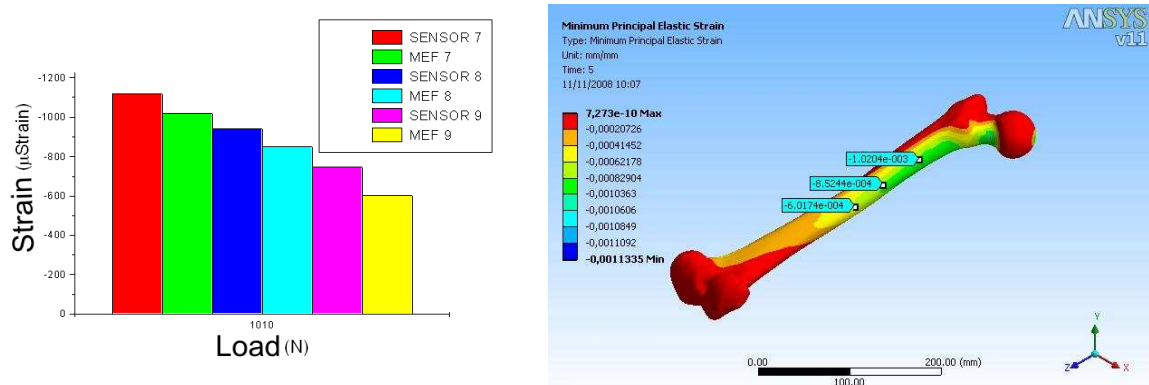


Figure 8: Strain in compression, at the medial face of femur.

Sensor 8, located at the medial part of the osteosynthesis plate, had strains of about  $1100 \mu\epsilon$ ; already for the same region, when simulated with FEM, the strain obtained was about  $450 \mu\epsilon$ . The highest differences between the two methods of are related to the fixation form and number of screws used.

Using eight screws, the distribution of the strains are concentrated in eight different points. In the numerical modeling, the strains are concentrated at the interface between the osteosynthesis plate and femur. This is the main factor affecting the strains at the body of the plate.

In both methods of fixation of the plate (numerical or experimental models), the strains are concentrated mainly at the medial part of the plate, due to presence of the space between the bone fragments. At the superior part as in the inferior part of the plate, the strains are low. These results are very similar as in the FEM as in experimental models, with use of the FBG, mainly the behaviors of the curves presented in graphs. The results obtained in the present work are very similar to ones obtained by Talaia, 2007, where there are strains around  $400 \mu\epsilon$  at the medial part of the plate and very small strains (below of the  $100 \mu\epsilon$ ) at the inferior and superior parts. This demonstrates that there are agreement between this study and others reported in literature.

The geometry of osteosynthesis plates induces the concentrations of strains around the holes. To demonstrate this behavior of strains, an image (fig. 9) with detail was taken, where the strain values around the holes are listed as well as in a horizontal line, between holes.

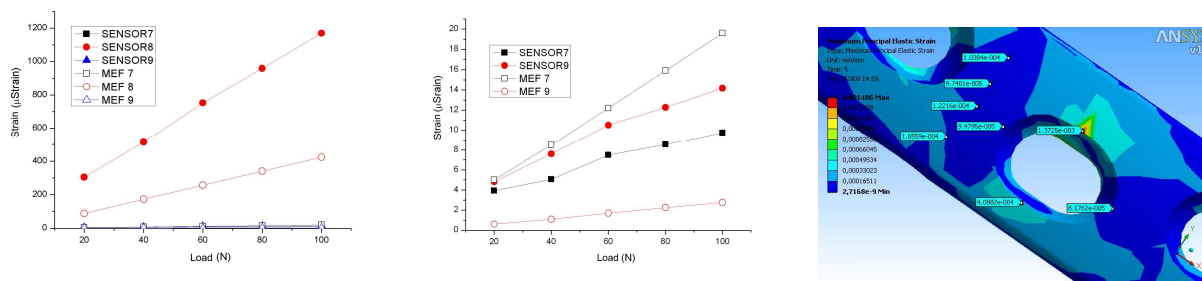


Figure 9: Comparison of strains, between the numerical and experimental models, at the osteosynthesis plate; at the extreme of the plate; and maximum principle strains at the plate, after load.

When considering the strains around the hole (located at the fracture region, therefore without the presence of screw), the value arises up to  $1372 \mu\epsilon$  and in the region, between the holes, and the strains are between  $97 \mu\epsilon$  and  $150 \mu\epsilon$ . It can be seen that a variation in the longitudinal positioning of the plate about 1 or 2 mm, can modify significantly the intensity of strains at the fracture location, after fixation. The present model does not take into account this type of analysis, therefore is considered an empty space between the fragments of the fracture. It would be very interesting, therefore, considering, in the model, the existence of a substance between the fragments, and therefore the levels of strains could be assessed at the focus of the fracture and then would be possible to clearly identify at what point of the window of the mecanostatic theory of Frost these situations are.

#### 4. CONCLUSIONS

With the present work, it was possible to improve the geometry. The objective of the present work was the validation of a numerical model of a synthetic femur and was achieved. The experimental results were in accordance with ones obtained in previous works, developed at the University of Aveiro by Talaia, 2007, and Ramos, 2006, with synthetic femur developed by SAWBONES<sup>®</sup>. However, in this work, it was developed a new support system for the experimental set up, in order to approach a more physiological behavior of applied loads and to refine the numerical model.

The results evidence that the regions of higher strain values are around holes, at the plate. Around the hole located at the focus of the fracture, therefore without the presence of screw, were observed the highest values of strain. A little variation in the position of osteosynthesis plates, around 1 or 2 mm, can interfere drastically in the strain level at the focus of the fracture, conditioning the efficiency of healing process.

The use of FBG as sensory systems for strain analysis at bone surfaces is very promising. They are able to be glued in irregular surfaces and geometries. The multiplexation of several sensors in the same optical fiber is a very interesting issue for the choice of a proper acquisition system, compared with other ones like strain gauges.

#### 3. ACKNOWLEDGEMENTS

This work was supported by the CNPq (471139/2007-6), plus CAPES and the Fundação Araucária for the support of the laboratory. Biomechanics Research Group of the University of Aveiro is thanked for supporting the research to develop the geometry of the numerical model.

#### 4. REFERENCES

- Argenta, M.A., Almeida, F.R., Karam, L.Z., 2008, "Methodology for Modeling and Analysis of Biological Structures Using Ansys Workbench", Ansys User's Conference, Rio de Janeiro.
- Carrer, J.A.M., 2006, "Introdução aos Métodos Aproximados em Engenharia. Texto Técnico", Programa de Pós-Graduação em Métodos Numéricos, CESEC, UFPR.
- Chong, A.C., Friis, E.A., Ballard, G.P., Czuwala, P.J., Cooke, F.W., 2007, "Fatigue performance of composite analogue femur constructs under high activity loading", *Annals of Biomedical Engineering*, 35(7):1196-205.
- Chong, A.C.M., Miller F., Buxton M., Friis E.A., 2007, "Fracture Toughness and Fatigue Crack Propagation Rate of Short Fiber Reinforced Epoxy Composites for Analogue Cortical Bone", *J. Biomech. Eng.*, Volume 129, Issue 4, 487:493.
- Hill, K.O., Fujii, Y., Johnson, D.C., Kawasaki, B.S., 1978, "Photosensitivity In Optical Fiber Waveguides: Application to Reflection Filter Fabrication", *Applied Physics Letters*, 32, 647-649.
- Huiskes R., Chao, E.Y.S., 1983, "A Survey Of Finite Element Analysis In Orthopaedic Biomechanics: The First Decade", *Journal of Biomechanics*, 16: 385-409.
- Kelly, K., 1998, "The Third Culture", *Science*, 179:192-193.
- Kersey, A.D., Davis, M.A., Patrick, H.J., Leblanc, M., Koo, K.P., Askins, C.G., Putnan, M.A., E.J. Friebele, 1997, "Fiber Grating Sensor", *Journal of Lightwave Technology*, 15, 1442-1462.
- Mcnamara, B.P., Cristofolini L., Toni A., Taylor D., 1997, "Relationship between Boneprosthesis Bonding and Load Transfer in Total Hip Reconstruction". *J Biomech*, 30(6):621-30.
- Mehlman C, OAS, D., 2006, "Biomechanical Comparison of Retrograde Elastic Stable Intramedullary Nailing Versus Locked Bridge Plating for Comminuted Pediatric Femoral Shaft Fractures Using a Synthetic Bone Model", *Orthopaedic Trauma Association, Scientific Poster #49 Pediatrics*, 377.
- Othonos, A., Kalli, K., 1999, "Fiber Bragg Grating: Fundamentals and Applications in Telecommunications and Sensing". London: Artech House.
- Prendergast, P.J., 1997, "Finite Element Models In Tissue Mechanics And Orthopaedic Implants Design", *Clinical Biomechanics*, 12: 343-366.
- Prendergast, P.J. Van Driel, W.D And Kuiper, J.H., 1996, "A Comparison Of Finite Element Codes For The Solution Of Biphasic Poroelastic Problems", *Process Of Instrumental Mechanical Engineerings*, 210: 131-136.
- Ramos, A., Simões, J.A., 2005, "Validação Experimental de um Modelo Numérico de um Fémur sintético Usado no Projecto de Próteses de Anca", *Mecânica Experimental*, 11, pp. 101-10.
- Roux, W., 1881, "Der Kampf der Theile im Organismus", Engelmann, Leipzig.
- Ruedi, T.P. e Murphy, W.M., 2002, "Princípios AO do Tratamento de Fraturas". Porto Alegre, Artmed Editora S.A.
- Talaia, P.M., Ramos, A., Abe, I., Schiller, M.W., Lopes, P., Nogueira, R.N., Pinto, J.L., Claramunt, R., Simões, J.A., 2007, "Plated and Intact Femur Strains in Fracture Fixation Using Fiber Bragg Gratings and Strain Gauges", *Experimental Mechanics*, 47:355-363.
- Wolff, J., 1892, "Das geset der transformation der knochen" (translated as 'the law of bone remodeling' by P. Maquet and R. Furlong), 1986, Springer, Berlin, Hirchwild (1892).
- Wu, J.Z., Herzog, W. And Epstein, M. , 1998, "Evaluation Of The Finite Element Software Abaqus For Biomechanical Modeling Of Biphasic Tissues", *Journal of Biomechanics*, 31: 165-169.
- Zhang, J., Jin, G.C., Meng, L.B., Jian, L.H., Wang, A.Y., Lu, S.B., 2005, "Strain and Mechanical Behavior Measurements of Soft Tissues with Digital Speckle Method", *Journal of biomedical optics* 10(3):034021.

#### 5. RESPONSIBILITY NOTICE

The authors are the only responsible for the printed material included in this paper.